Int. J. Heat Mass Transfer. Vol. 33, No. 9, pp. 1957–1968, 1990
Printed in Great Britain

0017-9310/90 $3.00 + 0.00

Effects of internal radiative transfer on natural convection and heat transfer in a vertical crystal growth configuration

H. MATSUSHIMA† and R. VISKANTA
Heat Transfer Laboratory, School of Mechanical Engineering, Purdue University, West Lafayette, IN 47907, U.S.A.

(*Received* 7 *August* 1989 *and in final form* 8 *November* 1989)

Abstract—The paper examines the effect of internal radiation on the process of growing a single crystal. A two-dimensional model of the vertical growth configuration is used to simulate the vertical Bridgman method. The differential approximation is used to model radiative transfer on the spectral basis and account for interactions within the crystal and the melt. Boundary conditions for semitransparent crystals which cover the range from opaque to transparent are developed. The governing model equations are solved numerically using a finite-difference method. The solutions show the notable reduction of the temperature difference near the crystal–melt interface and of the intensity of natural convection in the melt with the decrease in the opacity of the crystal. Radiation from the sidewall is found to be a factor in influencing the natural convection flow structure in the melt. The calculations show that there is relatively little difference between the spectral-band predictions and the gray model results based on the geometric mean absorption coefficient. The results obtained indicate the necessity to consider internal radiative transfer for improving the accuracy of models to simulate single crystal growth.

INTRODUCTION

MODERN communication and computer electronics is based on the manufacture of semiconductor devices on microscale. The reliable performance of these devices with dimensions less than 1 μm is strongly dependent on the quality of the single semiconductor crystals. One of today's most important problems in growing large semiconductor crystals, e.g. Si, GaAs, InP, is the homogeneity of the electrical resistivity on the microscale.

It is well established that convection in the melt or solution can affect the quality of the crystal [1] and that there does not exist a single cause but a multiplicity of possible reasons which can lead to unstable growth conditions and inhomogeneity in crystals. Convective flow and heat transfer during the growth of crystals from the melt has received considerable research attention, but the understanding of the processes and modeling capability is lagging behind the practical achievements in crystal growth technology.

There are many different types of crystal growth techniques [1]. Among those most commonly used are the vertical crystal growth configurations such as the Czochralski, vertical Bridgman and vertical zone melting methods. Many models have been developed and reported in the literature to simulate crystal growth processes mathematically [2, 3]. Radiation heat transfer at high temperature growth conditions may be important in both the crystal and the melt; however, radiation is typically ignored or when it is considered [4] it is treated as a surface and not a bulk (volumetric) phenomenon. Radiation has been recognized for some time as an important transport process during crystal growth [5, 6]. The temperature distribution in the melt near the crystal–melt interface is determined by the interaction of convection and radiation and in the solid by the interaction of conduction and radiation. Yuferev and Vasil'ev [7] have discussed the effect of radiation in semitransparent crystals grown from melt and have shown that the presence of a supercooled region close to the melt meniscus can lead to the instability of the crystallization front and the formation of a cellular interface boundary.

The common semiconductor crystals are not opaque to radiation. The spectral absorption coefficient of silicon and gallium-arsenide crystals, for example, depend strongly on the free-carrier concentration [8, 9]. The results show that pure silicon has a strong absorption band in the spectral range between 1 and 16 μm, but is relatively weakly absorbing in the wings of the band. The absorption coefficients of Si, GaAs and other semiconductors increases dramatically with the dopant concentration, but the crystal still remains semitransparent and not opaque [8, 9]. When both the crystal and the melt are semitransparent, thermal radiation is expected to interact with conduction and/or convection and affect the temperature distribution near the crystallization front and influence the quality of the crystal.

† Present address: Mechanical Engineering Research Laboratory, Hitachi, Ltd., 502 Kandatsu-machi, Tsuchiura-shi, Ibaraki 300, Japan.

NOMENCLATURE

c	specific heat of the melt [J kg^{-1} K^{-1}]
$E_{b\lambda}$	spectral black body emitted flux by Planck's law [W m^{-2} μm^{-1}]
g	gravitational acceleration [m^2 s^{-1}]
H	height of the domain (see Fig. 1) [m]
h_{eff}	effective heat transfer coefficient for cooling [W m^{-2} K^{-1}]
J_λ	spectral irradiance [W m^{-2} μm^{-1}]
k	thermal conductivity [W m^{-1} K^{-1}]
L	width of the domain (see Fig. 1) [m]
N	conduction–radiation interaction parameter, $\kappa_m k/n^2\sigma T_0^3$
P	pressure [N m^{-2}]
$q_{r,i}$	i-component of the radiative heat flux [W m^{-2}]
Ra	Rayleigh number, $g\beta\Delta TL^3/\alpha\nu$
T	temperature [K]
T_{ref}	reference temperature for natural convection, $(T_H+T_f)/2$ [K]
T_0	reference temperature, T_f [K]
u	x-component of velocity [m s^{-1}]
v	y-component of velocity [m s^{-1}]
x	horizontal coordinate [m]
y	vertical coordinate [m].
κ_m	geometric mean absorption coefficient, $\sqrt{(\kappa_P\kappa_R)}$ [m^{-1}]
κ_P	Planck mean absorption coefficient [m^{-1}]
κ_R	Rosseland mean absorption coefficient [m^{-1}]
κ_λ	spectral absorption coefficient [m^{-1}]
λ_j	mean wavelength at band center [μm]
$\Delta\lambda_j$	width of band j [μm]
μ	dynamic viscosity of the melt [kg m^{-1} s^{-1}]
ν	kinematic viscosity of the melt [m^2 s^{-1}]
ρ	reflectivity of the crucible wall
ρ_s	reflectivity of the crystal boundary
ρ_0	density of the melt [kg m^{-3}]
ρ_∞	reflectivity of the surrounding (heat source) wall
σ	Stefan–Boltzmann constant
τ_w	transmissivity of the crucible wall
τ_{ws}	transmissivity of the crystal boundary
τ_0	opacity of the crystal, $\kappa_m H$
ϕ	parameter, $\varepsilon_w/2(2-\varepsilon_w)$
ϕ_s	parameter, $\varepsilon_{ws}/2(2-\varepsilon_{ws})$.

Greek symbols

α	thermal diffusivity [m^2 s^{-1}]
β	thermal expansion coefficient [K^{-1}]
ε_w	emissivity of the crucible wall
ε_{ws}	emissivity of the crystal boundary
ε_∞	emissivity of the surrounding (heat source) wall

Subscripts

C	cold
f	fusion
H	hot
s	crystal.

The purpose of this paper is to study the effect of internal radiative transfer in the crystal and melt on the temperature distributions in the crystal and the melt and on the flow structure in the melt for a vertical crystal growth configuration. The intent here is not to simulate realistically the system but to assess the relative importance of internal radiative transfer in comparison to other modes of energy transport. A two-dimensional model is considered to simulate the most important heat transfer processes in a vertical Bridgman crystal growth facility. The differential approximation is used to model radiative transfer in the crystal and the melt. Radiation heat transfer across the crystal–melt interface is also accounted for. The spectral absorption coefficient and thermal conductivity of semiconductors at high temperatures are not known with sufficient accuracy to warrant use of rigorous formulation of radiative transfer in an axisymmetric geometry as is typical of the vertical Bridgman growth configuration. Silicon is taken as a semiconductor, and the model parameters for this study are assumed to be representative of its growth. Calculations have been performed for a range of optical dimensions to examine the importance of radiation vs conduction in the crystal and the importance of radiation vs convection in the melt on the flow and temperature structures.

ANALYSIS

Physical model and assumptions

The physical model and coordinate system of the problem are illustrated schematically in Fig. 1. In this study two physical situations are considered. The melt is heated from the bottom by imposing a constant and uniform temperature T_H at the bottom of the crucible. The crystal–melt interface is assumed to be at the equilibrium melting temperature T_f. The crystal is cooled at the top by combined convection and radiation. To facilitate the analysis this cooling is characterized by an effective heat tansfer coefficient $\tilde{h}_{eff}$ and temperature T_C. In Fig. 1(a), the crucible walls are assumed to be adiabatic, while in Fig. 1(b) the vertical walls are assumed to be semitransparent

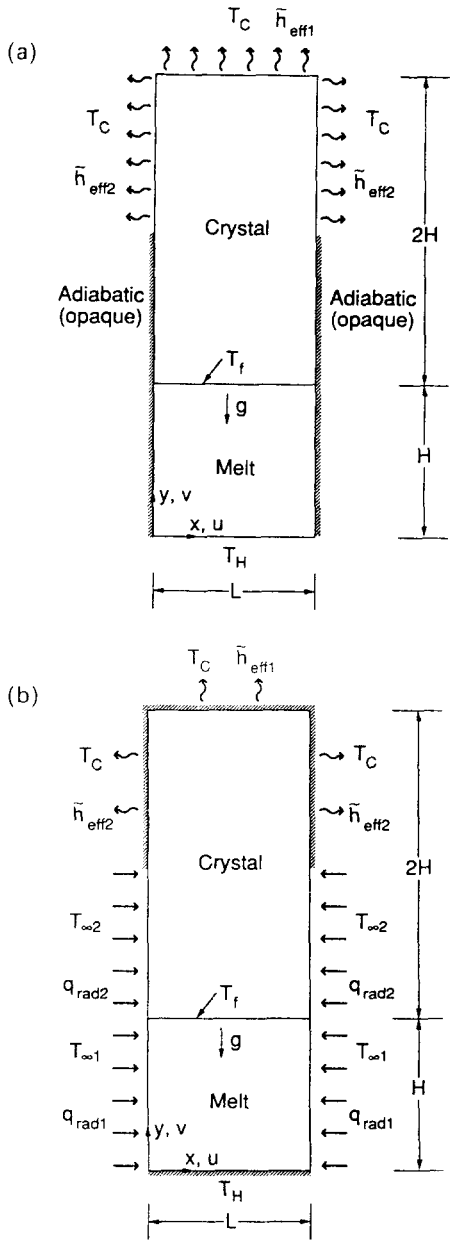

FIG. 1. Schematic of the physical model and coordinate system: (a) opaque sidewalls; (b) semitransparent sidewalls.

(quartz) and are heated by radiation from a heater (source at an effective temperature $T_{\infty 2}$). In Fig. 1(b), the lower portion of the semitransparent crystal is heated by radiation from an external source characterized by temperature $T_{\infty 1}$. Even though the actual temperature of the external source may vary along the height, the stepwise change of an effective temperature is assumed for the purpose of simplicity.

The melt is considered to be an incompressible, Newtonian fluid for which the Boussinesq approximation is valid. Viscous heat dissipation in the melt is neglected. The crystal growth front velocity is negligibly small compared to a characteristic convection velocity so that the flow and heat transfer can be considered steady. Hence, the crystallization front is fixed. The flow in the melt is laminar. Spectral radiative transfer in the semitransparent crystal and melt is approximated using a differential (P_1 or Milne-Eddington) approximation [10, 11]. Rigorous formulation of spectral radiative transfer is feasible [12], but does not appear to be warranted at the present time, because the spectral absorption coefficients and indices of refraction of the crystal and the melt are not known at temperatures and dopant concentrations corresponding to typical growth conditions. The thermophysical and radiative properties are assumed to be known and independent of temperature.

Taking advantage of the assumptions, the governing equations for the transport of mass, momentum, energy and spectral radiation in the melt and crystal can be expressed as:

for melt

$$\frac{\partial u}{\partial x}+\frac{\partial v}{\partial y}=0 \tag{1}$$

$$\rho\left(u\frac{\partial u}{\partial x}+v\frac{\partial u}{\partial y}\right)=\mu\left(\frac{\partial^2 u}{\partial x^2}+\frac{\partial^2 u}{\partial y^2}\right) \tag{2}$$

$$\rho\left(u\frac{\partial v}{\partial x}+v\frac{\partial v}{\partial y}\right)=-\frac{\partial P}{\partial y}+\mu\left(\frac{\partial^2 v}{\partial x^2}+\frac{\partial^2 v}{\partial y^2}\right)+\rho g\beta(T-T_{ref}) \tag{3}$$

$$\rho c\left(u\frac{\partial T}{\partial x}+v\frac{\partial T}{\partial y}\right)=k\left(\frac{\partial^2 T}{\partial x^2}+\frac{\partial^2 T}{\partial y^2}\right)+\int_0^\infty \kappa_\lambda(J_\lambda-E_{b\lambda})\,d\lambda \tag{4}$$

$$\frac{\partial^2 J_\lambda}{\partial x^2}+\frac{\partial^2 J_\lambda}{\partial y^2}=3\kappa_\lambda^2(J_\lambda-E_{b\lambda}); \tag{5}$$

for crystal

$$k_s\left(\frac{\partial^2 T_s}{\partial x^2}+\frac{\partial^2 T_s}{\partial y^2}\right)+\int_0^\infty \kappa_{\lambda s}(J_{\lambda s}-E_{b\lambda s})\,d\lambda=0 \tag{6}$$

$$\frac{\partial^2 J_{\lambda s}}{\partial x^2}+\frac{\partial^2 J_{\lambda s}}{\partial y^2}=3\kappa_{\lambda s}^2(J_{\lambda s}-E_{b\lambda s}). \tag{7}$$

The radiative heat fluxes in the x- and y-directions are related to the irradiance J_λ by

$$q_{r,x}=-\int_0^\infty \frac{1}{3\kappa_\lambda}\frac{\partial J_\lambda}{\partial x}\,d\lambda \quad \text{and} \quad q_{r,y}=-\int_0^\infty \frac{1}{3\kappa_\lambda}\frac{\partial J_\lambda}{\partial y}\,d\lambda. \tag{8}$$

The boundary conditions for the physical model shown in Fig. 1(a) are taken to be as follows:

momentum

$$u=v=0 \quad \text{at the walls and interface in the melt;} \tag{9}$$

energy

$$T = T_H \quad \text{at the bottom} \quad (y = 0) \tag{10}$$

$$k\frac{\partial T}{\partial y} + \int_0^\infty \frac{1}{3\kappa_\lambda}\frac{\partial J_\lambda}{\partial y}\,d\lambda = k_s\frac{\partial T_s}{\partial y} + \int_0^\infty \frac{1}{3\kappa_{\lambda s}}\frac{\partial J_{\lambda s}}{\partial y}\,d\lambda$$

at the crystal–melt interface (11)

$$-k_s\frac{\partial T}{\partial x} = h_{eff}(T_C - T_w) + \int_0^\infty \phi_s(J_{w\lambda} - E_{bw\lambda})\,d\lambda$$

at the cooled wall (12)

$$-k\frac{\partial T}{\partial x} = \int_0^\infty \phi(J_{w\lambda} - E_{bw\lambda})\,d\lambda$$

at the adiabatic wall; (13)

radiative transfer

$$\frac{\partial J_\lambda}{\partial x_i} = 3\kappa_\lambda\phi(J_{w\lambda} - E_{bw\lambda}) \quad \text{at the opaque wall.} \tag{14}$$

The boundary conditions for temperature and irradiance at the semitransparent crystal boundary (Fig. 1(b)) have also been derived. The interreflections between the crystal boundary and the surrounding heater (assumed to be planar, gray and opaque at a prescribed temperature) have been accounted for. The details are not interesting, the equations are rather complex, and are therefore not included in the paper. The procedure described in graduate level radiation heat transfer textbooks [13] was followed to account for the interreflections between the crystal boundary and the opaque crucible walls. The boundary conditions for radiative transfer corresponding to the model described in Fig. 1(b) are available elsewhere [14]. For the limiting cases of an opaque crucible wall ($\rho + \varepsilon_w = 1$) and a transparent crucible wall ($\rho + \tau_w = 1$) with black surroundings, the equations obtained in this study reduce to those developed by Amlin and Korpela [11].

Method of solution

The model equations together with the boundary conditions were solved numerically using a finite-difference method. The control volume scheme of Patankar [15] was used to reduce the system of governing partial differential equations to a set of nominally linear algebraic equations. The SIMPLER algorithm was employed to treat the coupling between the pressure and momentum. Nodes were clustered near the walls, crystal–melt interface and boundaries to accurately calculate the large velocity, temperature and irradiance gradients. A power law clustering scheme was used for this purpose. Grid independence studies were conducted, and a final grid of 43 × 24 was chosen. The numerical results reported in the paper were obtained using this grid.

In the analysis, the spectral absorption coefficient data for doped silicon were taken from the literature [8]. The specific data used as an example are for p-type silicon of electrical resistivity of 0.5 Ω cm at 300 K. Data at higher temperature would be desirable for use in the analysis. Unfortunately, a literature source for such data could not be identified. For this reason the spectral absorption coefficients for the crystal and the melt are assumed to be identical.

The spectral integrations indicated in equations (4), (6), (8) and (11)–(13) were performed using a band approximation. The entire spectrum was divided into N arbitrary width bands to model the spectral absorption coefficient, and the integrals over the spectrum were approximated as

$$\int_0^\infty \kappa_\lambda J_\lambda\,d\lambda \cong \sum_{j=1}^{N} \kappa_{\lambda_j} J_{\lambda_j}\Delta\lambda_j. \tag{15}$$

It is highly desirable to compare the predictions of radiative transfer based on spectral-band calculations with those based on a gray analysis to determine the validity of the simplified approach. To examine the usefulness of such analysis we introduce mean absorption coefficients. The Planck, Rosseland and geometric mean absorption coefficients are defined as [12]

$$\kappa_P = \int_0^\infty \kappa_\lambda E_{b\lambda}(T)\,d\lambda \Big/ \int_0^\infty E_{b\lambda}(T)\,d\lambda \tag{16}$$

$$1/\kappa_R = \int_0^\infty \frac{1}{\kappa_\lambda}\frac{dE_{b\lambda}}{dT}\,d\lambda \Big/ \int_0^\infty \frac{dE_{b\lambda}}{dT}\,d\lambda \tag{17}$$

and

$$\kappa_m = (\kappa_P\kappa_R)^{1/2} \tag{18}$$

respectively.

The Planck and Rosseland mean absorption coefficients were calculated using the melting temperature (1685 K) of silicon as the reference temperature. The values found for the mean absorption coefficients using the specific data and used in the computations for comparison were as follows:

$$\kappa_P = 141\,m^{-1}, \quad \kappa_R = 61.6\,m^{-1}$$

and $\kappa_m = 93.2\,m^{-1}$.

RESULTS AND DISCUSSION

There are many parameters affecting the transport processes modeled. Since the primary focus of the work is on radiative transfer and its interaction with other modes of heat transfer during crystal growth, representative values of parameters have been chosen to simulate the system. The thermophysical properties and other dimensionless parameters used in the sample calculations are summarized in Table 1. The Rayleigh number was kept fixed at a typical value of $Ra = 1 \times 10^5$ for most cases, unless indicated otherwise.

In crystal growth facilities the aspect ratio H/L changes with time, but the change is relatively slow. The range of the ratio which is encountered in practice is between 0.5 and 5, and $H/L = 1$ is considered a typical value [16]. By considering the crystal and melt regions, a fixed value of two for the height ratio of the crystal to melt region was considered to be reasonable

Table 1. Thermophysical properties and dimensionless model parameters used for the spectral-band calculations. To obtain the gray model results in Fig. 1(b) the values given in parentheses were used

$Gr = 4.35 \times 10^6$	$\phi = \phi_s = 0.088$
$Pr = 0.023$	$h_{eff1} = 350\ W\ m^{-2}\ K^{-1}$
$n = 3.4$	$h_{eff2} = 175\ W\ m^{-2}\ K^{-1}$
$k = 52\ W\ m^{-1}\ K^{-1}$	$T_f = 1685\ K$
$k_s = 22\ W\ m^{-1}\ K^{-1}$	$T_H = 1695\ K$
$\beta = 2 \times 10^{-4}\ K^{-1}$	$T_C = 1520\ K\ (1200\ K)$
$\rho_0 = 2550\ kg\ m^{-3}$	$L = 0.0301\ m$
$\alpha = 1.53 \times 10^{-5}\ m^2\ s^{-1}$	$H = 0.0301\ m$
$\nu = 3.5 \times 10^{-7}\ m^2\ s^{-1}$	$(T_{s,1} = 1695\ K)$
$T_{ref} = 1690\ K$	$(T_{s,2} = 1685\ K)$

and was used in the calculations. This is not a limitation of the model, but the sensitivity of the results to this ratio and other important model parameters such as the thermal conductivities of crystal and melt, absorption coefficients of crystal and melt, radiation surface properties and others could not be investigated in detail. For example, the thermal conductivities used in the sample calculations (see Table 1) were taken from the published literature sources. However, it is not clear if these are true thermal conductivities or are actually effective thermal conductivities, because they were not corrected for the contribution of radiation when making the measurements, particularly at elevated temperatures [12].

Absence of internal radiative transfer

In order to establish a base, internal radiative transfer was neglected, and the flow structure in the melt and the temperature distribution in both the melt and the crystal were predicted. The results are shown in Fig. 2. The calculations were initiated from stagnant melt and uniform temperature conditions. The results show that the flow is symmetrical about the vertical plane through the center of the melt forming two counter rotating cells (Fig. 2). Even though not evident from Fig. 2(b), small recirculation cells in the four corners of this melt region are present. This is typical of low Prandtl number fluids [17]. The isotherms are spaced rather uniformly in the crystal, particularly near the crystallization front, which indicates nearly constant temperature gradients. The nonuniformly spaced isotherms in the melt reveal the importance of convection in the transport of heat. As expected, the temperature gradients in the melt near the center of the crystal are greater than near the edges.

Internal radiative transfer: spectral-band analysis

The streamlines in the melt and the isotherms in both the crystal and the melt when the spectral effects of internal radiation transfer have been considered using the model in Fig. 1(a) are presented in Fig. 3 and the heat fluxes in Figs. 4 and 5. The corresponding results of gray calculations (Figs. 6 and 7) will be discussed later. The results of this simulation should be compared with those given in Fig. 6 for $\tau_0 = 2.8$. The spectral-band calculations show that thermal convection in the melt is somewhat more intense ($\psi_{max} = 0.145\ kg\ s^{-1}$) than those based on the gray absorption coefficient model ($\psi_{max} = 0.134\ kg\ s^{-1}$). The two-cell circulation pattern is practically the same.

Comparison of temperature distributions calculated using the spectral-band (Fig. 3(b)) and the gray (Fig. 6(b)) models for the absorption coefficient shows that the temperature gradients in the vertical

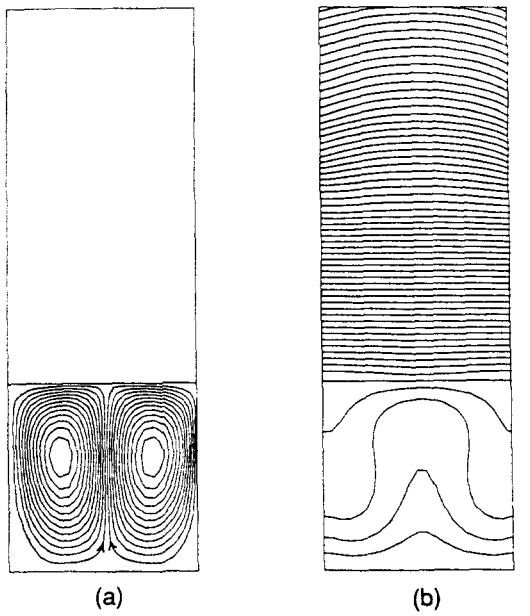

FIG. 2. Streamlines (a) in the melt and isotherms (b) in the melt and crystal in the absence of internal radiative transfer. The isotherm spacing is 2 K.

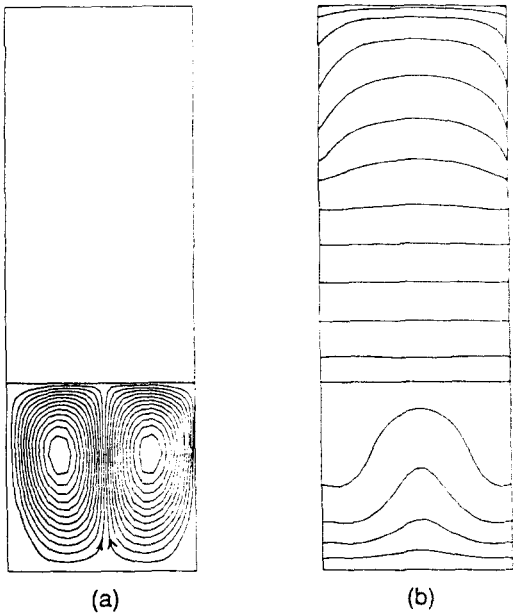

FIG. 3. Streamlines (a) in the melt and isotherms (b) in the melt and crystal in the presence of internal radiative transfer, spectral-band model for absorption coefficient.

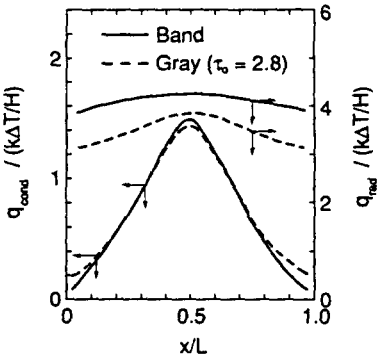

FIG. 4. Comparison of the local conductive and radiative heat fluxes at the crystal–melt interface for the gray and spectral-band absorption coefficient models.

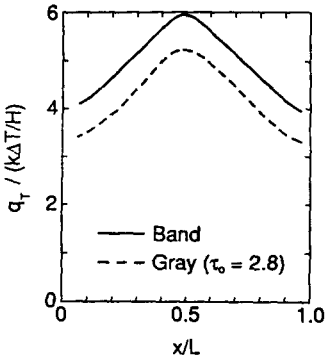

FIG. 5. Comparison of the total (conductive plus radiative) heat fluxes at the crystal–melt interface for the gray and spectral-band absorption coefficient models.

and horizontal directions in the melt are larger for the former than the latter model. However, the results reveal that the temperature gradients in the crystal are smaller for the spectral-band than for the gray analysis.

A comparison of the conductive and radiative heat fluxes at the crystal–melt interface for the spectral-band and gray absorption coefficient models is given in Fig. 4. The results show that the maximum conductive flux is about three times smaller than the maximum radiative flux. This clearly shows the importance of internal radiative vs diffusive transfer. It should be mentioned that the thermal conductivities for silicon reported in the literature were used in the calculations. If, in reality, these values are effective thermal conductivities which have not been corrected for internal radiative transfer, then the relative importance of radiation in comparison to conduction has been underpredicted. The local conductive flux is seen to be much more nonuniform than the local radiative flux. The conductive fluxes are nearly equal, except at the edges of the crystal where they differ significantly, but the radiative flux is about 25% greater for the spectral-band absorption coefficient model. Figure 5 shows that the total (conductive plus radiative) flux at the interface is relatively uniform and that the predicted flux is at least 15% higher for the spectral-band than the gray absorption coefficient models.

The difference between the spectral-band and gray model results based on the geometric mean absorption coefficient for the conductive and total heat fluxes are about 10 and 15%, respectively. The agreement

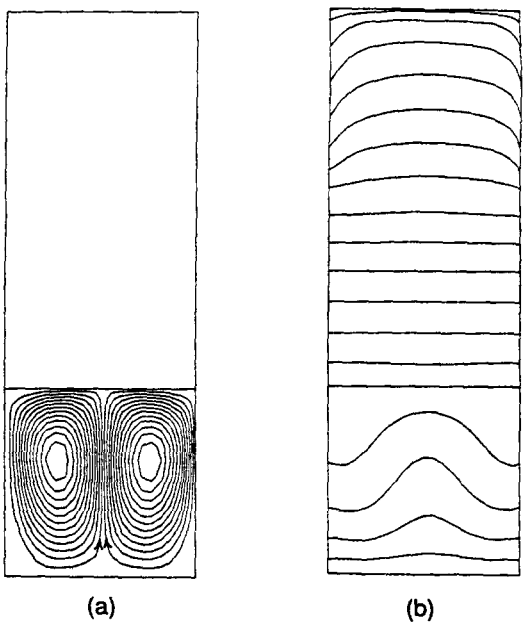

FIG. 6. Streamlines (a) in the melt and isotherms (b) in the melt and crystal in the presence of internal radiative transfer for opaque, adiabatic walls (Fig. 1(a)); gray absorption coefficient model, $\tau_0 = 2.8$. The isotherms are spaced 2 K apart.

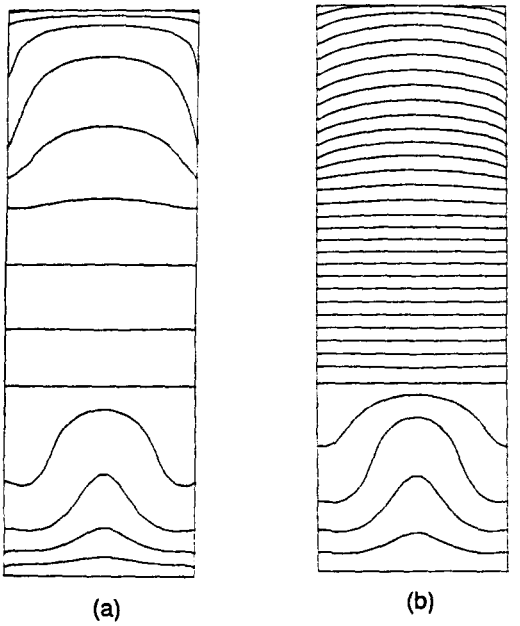

FIG. 7. Isotherms in the melt and crystal in the presence of internal radiative transfer, gray absorption coefficient model for opaque, adiabatic walls (Fig. 1(a)): (a) $\tau_0 = 1.0$; (b) $\tau_0 = 10$. The isotherms are spaced 2 K apart.

between the streamlines and isotherms for the two absorption coefficient models is resonable enough to encourage use of the gray model to examine the effect of internal radiative transfer on the flow and heat transfer in crystal growth systems.

Internal radiative transfer: gray model

Effect of opacity. The effect of internal radiative transfer on the flow structure in the melt and on the temperature distributions in the melt and crystal were predicted on the gray basis, and the results for $\tau_0 = 1$, 2.8 and 10 are shown in Figs. 6 and 7. The flow is still symmetrical about the vertical plane through the center of the melt forming two cells (Fig. 6(a)); however, the intensity of thermal convection in the melt is reduced as evidenced by the maximum and minimum values of the stream functions. For example, even with $\tau_0 = 10$, $\psi_{max} = 0.178$ and $0.165\ \text{kg s}^{-1}$ in the absence and in the presence of internal radiative transfer in the melt, respectively. Radiative transfer in the melt reduces the horizontal temperature gradients within the region and decreases the intensity of natural convection. The results show that as the optical thickness (opacity) of the melt decreases, the maximum stream function (normalized by the value of the maximum stream function for the radiationless case) decreases and reaches a minimum at about $\tau_0 = 1$. This finding is understandable considering the fact that the radiative heat flux reaches its maximum value near $\tau_0 = 1$ [18].

Internal radiative transfer in the melt reduces both the vertical and horizontal temperature gradients. This is clearly evident from the comparison of the isotherms shown in Fig. 2(b) with those in Figs. 3(b), 6(b) and 7. The presence of radiation in the crystal reduces significantly the vertical temperature gradient in the crystal (Figs. 3(b), 6(b) and 7) compared to that in the absence of internal radiative transfer (Fig. 2(b)). This is true even for the case when the opacity of the crystal is quite large ($\tau_0 = \kappa_m H = 10$ as in Fig. 7(b)). The results of Fig. 7 show that the reduction of the vertical temperature gradients in the crystal is even greater for smaller values of the opacity τ_0 (Fig. 7(a)).

The variation of the conductive heat flux along the crystal–melt interface is shown in Fig. 8. The heat flux has been normalized with the flux obtained for the radiationless (pure conduction) two-cell case. A large reduction in the conductive flux compared to the radiationless case is evident from the figure when $\tau_0 = 1.0$. This suggests that under the crystal growth conditions considered in the model, the interaction between convection and radiation is significant, particularly for the intermediate values of the opacity. The results also suggest that radiation accounts for a large fraction of the heat transfer to the interface.

The results show that the semitransparency of the melt and crystal to thermal radiation greatly modifies the temperature distribution and magnitude of the net thermal fluxes in a growing crystal, particularly at temperature conditions studied in the paper. The results also reveal that the interface temperature gradients in the liquid are always less steep relative to the case when the melt and crystal are opaque or transparent for the same imposed thermal conditions. Employing the 'constitutional supercooling' concepts of Mullins and Sekerka [19], leads one to conclude that the solid–liquid interface of semitransparent materials will tend to be less resistant to cellular breakdown than purely conducting (transparent or opaque) materials. These conclusions should apply only at conditions when radiative transfer is important compared to conduction or convection.

Effect of external radiation. Figures 9–12 show the streamlines in the melt and the isotherms in both the melt and the crystal for the case when the sides of crystal and crucible are semitransparent and are irradiated from the surroundings as modeled in Fig. 1(b). The additional radiation parameters used are summarized in Table 2. When the opacity is large ($\tau_0 = 10$), radiant energy incident on the sides of the crucible is absorbed near the edges and increases the

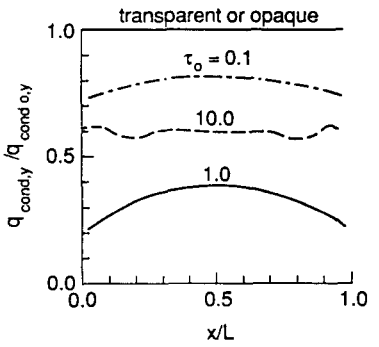

FIG. 8. Effect of internal radiative transfer on the variation of the local conductive heat flux at the crystal–melt interface for opaque, adiabatic walls (Fig. 1(a)).

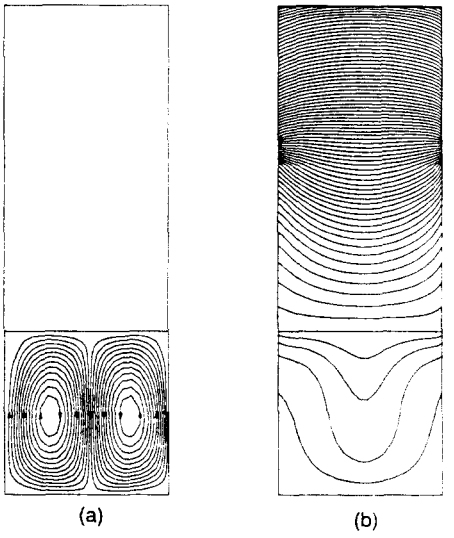

FIG. 9. Streamlines in the melt (a) and isotherms in the melt and crystal (b) for $Ra = 1 \times 10^5$ and $Pr = 0.023$ with externally irradiated vertical boundaries (model shown in Fig. 1(b)) and $\tau_0 = 10$ ($N = 0.551$).

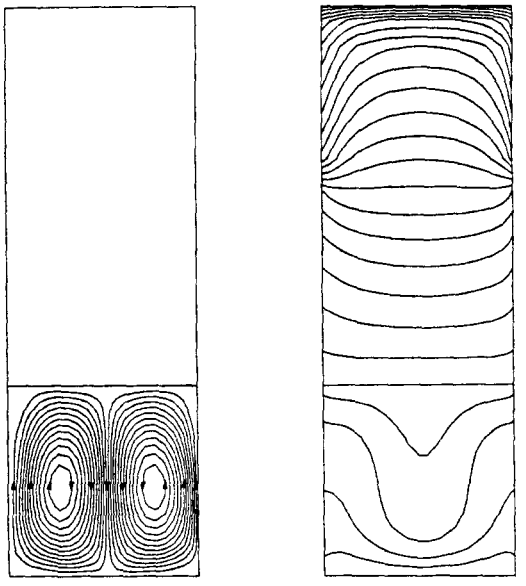

FIG. 10. Streamlines in the melt (a) and isotherms in the melt and crystal (b) for $Ra = 1 \times 10^5$ and $Pr = 0.023$ with externally irradiated vertical boundaries (model shown in Fig. 1(b)) and $\tau_0 = 1$ ($N = 5.51$).

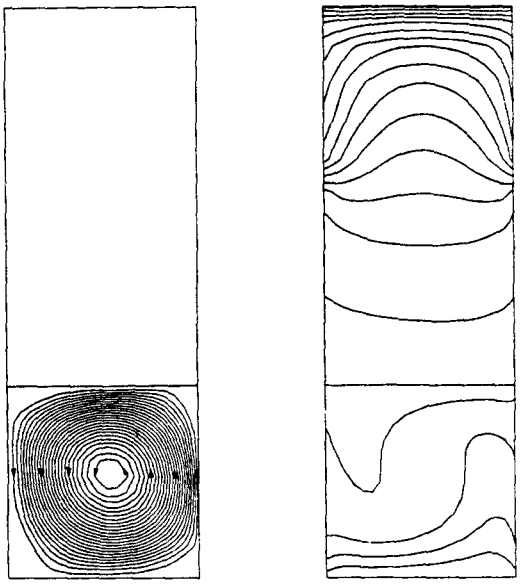

FIG. 12. Streamlines in the melt (a) and isotherms in the melt and crystal (b) for $Ra = 1 \times 10^5$ and $Pr = 0.023$ with externally irradiated vertical boundaries (model shown in Fig. 1(b)) and $\tau_0 = 0.175$ ($N = 0.0964$).

temperatures in this region. As a consequence, a two-cell flow pattern is established, with the fluid rising along the walls of the crucible and descending in the center of the melt region (Fig. 9(a)).

For the self-absorbing case ($\tau_0 = 1$) the effect of external radiation at the boundaries of the crucible are still strong (Fig. 10). The flow still consists of two cells and is symmetrical about a plane through the center of the melt region, but the dimensionless stream function decreases from 0.101 for $\tau_0 = 10$ to 0.094 for $\tau_0 = 1$. Comparison of Figs. 10 and 9 reveals that the temperature gradients have decreased dramatically for the smaller opacity case particularly in the crystal. This is due to the fact that radiation accounts for a much larger fraction of the total heat transfer along the crystal. Physically, this means that the radiation predominates over conduction. The findings are consistent with the results reported by Tarshis *et al.* [20].

There is a remarkable change in the flow structure in the melt (Fig. 11) for the optically thin case ($\tau_0 = 0.1$). The flow still consists of two cells and is symmetrical about the center plane; however, the direction of the circulation has been reversed compared to that predicted for larger opacities, but under otherwise identical thermal conditions (compare Figs. 9–11). This is explained by the fact that more radiant energy is absorbed in the central region of the melt resulting in higher temperatures in the center than near the walls of the crucible and the crystal boundaries, producing a higher temperature in the core which drives the thermal convective flow. The tem-

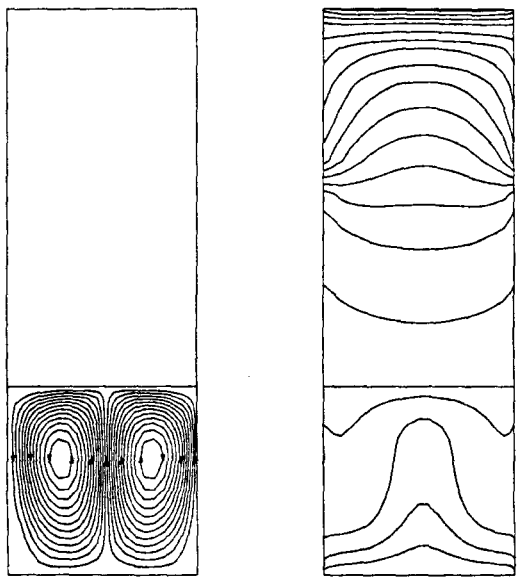

FIG. 11. Streamlines in the melt (a) and isotherms in the melt and crystal (b) for $Ra = 1 \times 10^5$ and $Pr = 0.023$ with externally irradiated vertical boundaries (model shown in Fig. 1(b)) and $\tau_0 = 0.1$ ($N = 0.551$).

Table 2. Radiation properties for the model shown in Fig. 2(b) for the simulations used with the gray model. For the baseline case the values in parentheses were used

$\varepsilon_w = 0.5$	$\rho_\infty = 0.05$ (1.0)
$\tau_w = 0.2$ (0)	$\varepsilon_\infty = 0.95$ (0)
$\tau_{ws} = 0.4$ (0)	$\varepsilon_{ws} = 0.3$
$\phi = 0.17$	$\rho = 0.3$ (0.5)
$\phi_s = 0.088$	$\rho_s = 0.3$ (0.7)

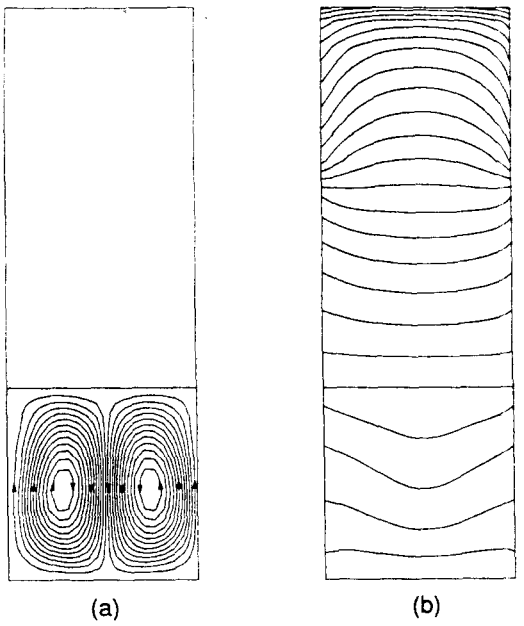

FIG. 13. Streamlines in the melt (a) and isotherms in the melt and crystal (b) for $\tau_0 = 1.0$ with externally irradiated vertical boundaries (model shown in Fig. 1(b)): $Ra = 1 \times 10^4$, $Pr = 0.023$, $N = 1.186$.

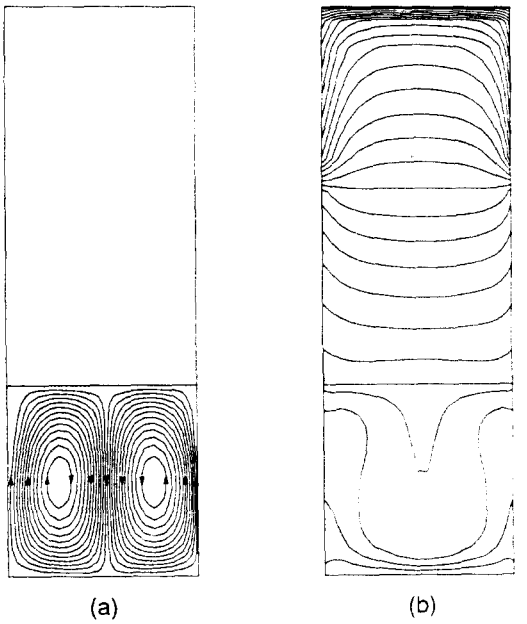

FIG. 14. Streamlines in the melt (a) and isotherms in the melt and crystal (b) for $\tau_0 = 1.0$ with externally irradiated vertical boundaries (model shown in Fig. 1(b)): $Ra = 1 \times 10^6$, $Pr = 0.023$, $N = 0.256$.

perature gradients along the crystal decrease further because of increased relative importance of radiation relative to conduction. It is recognized that the differential approximation for radiative transfer becomes increasingly more inaccurate as the opacity of the medium decreases. But even for an opacity of $\tau_0 = 0.1$, the approximation yields acceptable results (less than 15% error in the radiative flux in comparison to the exact solution) [21]; therefore, use of the approximation appears to be a reasonable compromise between accuracy and computational effort. This is particularly true in view of the acknowledged uncertainty in the physical and radiative properties of silicon crystal and melt at high temperatures.

It was found that for the particular thermal conditions imposed and model parameters chosen, there occurred a transition in the flow structure in the melt at an opacity of about 0.2. The streamlines and isotherms for $\tau_0 = 0.175$ are plotted in Fig. 12. It was found that there was no preference for a two-cell symmetrical downward or upward flow, and a single counterclockwise rotating cell was predicted. As expected, the temperature distributions in the melt for $\tau_0 = 0.1$ and 0.175 (compare Figs. 11 and 12) differed greatly, but the temperature distributions in the crystal near the interface was nearly identical.

Effect of Rayleigh number. The effect of the Rayleigh number on the flow and temperature distributions are shown in Figs. 13 and 14. In this calculation, the optical thickness ($\tau_0 = 1.0$) and all prescribed temperatures are kept the same as those for Fig. 10. Thus, only the size of the melt and crystal is changed. This alters the conduction–radiation parameter N along with the Rayleigh number.

Figure 13 illustrates the streamlines and isotherms for $Ra = 1 \times 10^4$. In this case, the intensity of natural convection (maximum stream function) has decreased and is 6.7 times lower than that for $Ra = 1 \times 10^5$ (Fig. 10). Thus, conduction and radiation predominate over convective heat transfer. For $Ra = 1 \times 10^6$ (shown in Fig. 14), natural convection is 3.3 times more intense than that for $Ra = 1 \times 10^5$ (Fig. 10), and convection and radiation are of equal importance in the melt.

Figure 15 shows the conductive heat flux at the crystal–melt interface. The heat flux is normalized with respect to pure conductive flux (absence of radiation and natural convection). The results reveal a large variation of the flux along the interface, with the maximum occurring near the walls and the minimum at the center. This is the result of natural convection in the melt, which intensifies with increasing Rayleigh

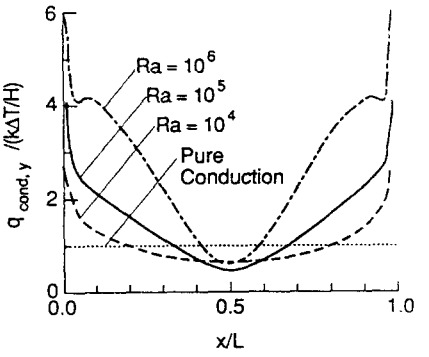

FIG. 15. Conductive heat flux at the crystal–melt interface: $\tau_0 = 1.0$ with externally irradiated vertical boundaries.

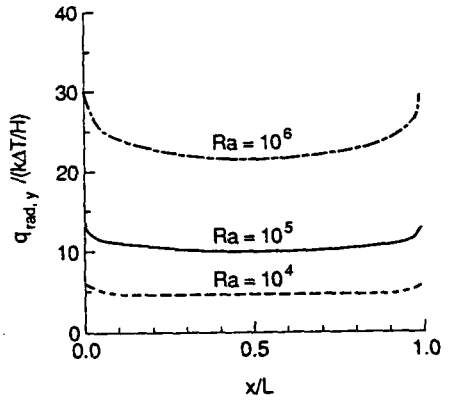

FIG. 16. Radiative heat flux at the crystal–melt interface: $\tau_0 = 1.0$ with externally irradiated vertical boundaries.

number. Thus, the local conductive heat flux at the crystal–melt interface is highly nonuniform, especially for higher Rayleigh numbers.

Figure 16 shows the radiative heat flux at the crystal–melt interface. The heat flux is also normalized using the pure conductive flux as in Fig. 15. A comparison of the radiative fluxes with the conductive heat fluxes (Fig. 15) reveals that the radiative heat flux is several times larger than the conductive flux, and its distribution along the interface is rather uniform. As a consequence, the total heat flux along the interface is also uniform in the presence of radiation. We should emphasize again that if the thermal conductivities of silicon at high temperature reported in the literature and used in the calculations have not been corrected for the internal radiative transfer effects, the relative importance of radiation vs conduction would be even greater than shown in Fig. 16. This further stresses the need for accurate thermophysical and radiative properties data of semiconductors at high temperatures.

CONCLUDING REMARKS

The effect of internal thermal radiation on the process of growing a single crystal has been investigated numerically. A two-dimensional model of a growth configuration is used to simulate the vertical Bridgman method. The differential approximation is used to model radiative transfer, and the interaction of convection with radiation in the melt as well as interaction of conduction and radiation in the crystal. Appropriate boundary conditions which allow for the transmission of external radiation across the boundaries have been derived. The governing model equations are solved numerically using both spectral-band and gray models for the absorption coefficient. Based on the numerical results obtained for silicon, the following conclusions are drawn.

It was found that there is relatively little difference between the spectral-band and gray results based on the geometric mean absorption coefficient. The gray analysis underpredicted the maximum conductive heat flux at the crystal–melt interface by less than 10% and the total heat flux by about 12–16%. The agreement between the streamlines and isotherms for the two absorption coefficient models is reasonable enough to encourage the use of the gray model when simulating flow and heat transfer in crystal growth systems.

The effect of internal thermal radiation on the flow structure and temperature distributions in the melt and in the crystal are most pronounced for intermediate values of opacity ($\tau_0 \cong 1$). For $\tau_0 = 1$ and $Ra = 1 \times 10^5$, the intensity of natural convection in the melt is reduced by about 20% compared to that for a transparent or opaque melt and crystal. The presence of internal radiative transfer is found to reduce the nonuniformity of temperature in both the melt and the crystal as well as of the total heat flux along the crystal–melt interface. The temperature gradients in the crystal decrease dramatically as the opacity of the crystal is decreased.

For small Rayleigh numbers conduction and radiation are of the same importance in establishing the temperature distribution. On the other hand, natural convection and radiation are the principal energy transport processes in the melt at high Rayleigh numbers. The presence of internal radiation is found to reduce the nonuniformity of the total heat flux along the crystal–melt interface.

The results obtained suggest that internal radiative transfer is a first-order effect and must be considered in both the melt and the crystal when mathematically modeling single crystal growth. For this purpose spectral absorption coefficient data as a function of temperature and impurity or dopant concentration is required not only for the crystal but also for the melt. A more rigorous formulation of radiative transfer than used in this paper will also be needed. Admittedly, such a formulation of radiative transfer for the Czochralski single crystal growth method will be exceedingly complex, but some reasonable approximations may be possible.

Acknowledgements—This work was done when one of us (H.M.) held a visiting research scholar appointment at Purdue University. He would like to express his appreciation to the Mechanical Engineering Research Laboratory, Hitachi, Ltd., for making his leave possible. Computing facilities were made available by Purdue University Computing Center.

REFERENCES

1. S. Ostrach, Fluid mechanics in crystal growth—The 1982 Freeman Scholar Lecture, *J. Fluids Engng* **105**, 5–20 (1983).
2. R. A. Brown, P. A. Sackinger, D. P. Thomas, J. J. Derby and L. J. Adornato, Application of large-scale simulation to materials processing: modelling of Czochralski growth single crystals. In *Interdisciplinary Issues in Materials Processing and Manufacturing* (Edited by S. K. Samanta, R. Komanduri, R. McMeeking,

M. M. Chen and A. Teng), Vol. 1, pp. 331–348. ASME, New York (1987).
3. H. Kopetsch, A numerical method for the time-dependent Stefan Czochralski crystal growth, *J. Crystal Growth* **88**, 71–86 (1988).
4. L. J. Atherton, J. J. Derby and R. A. Brown, Radiative heat exchange in Czochralski crystal growth, *J. Crystal Growth* **84**, 57–78 (1987).
5. S. O'Hara, L. A. Tarshis and R. Viskanta, Stability of the solid–liquid interface of semitransparent materials, *J. Crystal Growth* **3**, 583–593 (1968).
6. M. Abrams and R. Viskanta, The effects of radiative heat transfer upon the melting and solidification of semitransparent crystals, *J. Heat Transfer* **96**, 184–190 (1974).
7. V. S. Yuferev and M. G. Vasil'ev, Heat transfer in shaped thin-walled semi-transparent crystals pulled from the melt, *J. Crystal Growth* **82**, 31–38 (1987).
8. H. Wolf (Editor), *Silicon Semiconductor Data*. Pergamon Press, New York (1969).
9. E. D. Palik (Editor), *Handbook of Optical Constants of Solid*, p. 169. Academic Press, New York (1985).
10. S. C. Traugott, Radiative heat-flux potential for a nongray gas, *AIAA J.* **4**, 541–542 (1966).
11. D. W. Amlin and S. A. Korpela, Influence of thermal radiation on the temperature distribution in semitransparent solid, *J. Heat Transfer* **101**, 76–80 (1979).
12. R. Viskanta and E. E. Anderson, Heat transfer in semitransparent solids. In *Advances in Heat Transfer* (Edited by T. F. Irvine, Jr. and J. P. Hartnett), Vol. 11, pp. 317–441. Academic Press, New York (1975).
13. R. Siegel and J. R. Howell, *Thermal Radiation Heat Transfer* (2nd Edn). McGraw-Hill, New York (1981).
14. H. Matsushima and R. Viskanta, Effects of internal radiation on temperature distribution and natural convection in a vertical crystal growth configuration. In *Collected Papers in Heat Transfer 1988* (Edited by K. T. Yang), pp. 151–160. ASME, New York (1988).
15. S. V. Patankar, *Numerical Heat Transfer and Fluid Flow*. Hemisphere, Washington, DC (1980).
16. G. Müller, *Crystal Growth from the Melt*. Springer, Berlin (1988).
17. F. Wolff, C. Beckermann and R. Viskanta, Natural convection of liquid metals in vertical cavities, *Exp. Thermal Fluid Sci.* **1**, 83–91 (1988).
18. R. Viskanta, Interaction of heat transfer by conduction, convection and radiation in a radiating fluid. *J Heat Transfer* **85**, 318–328 (1963).
19. W. W. Mullins and R. F. Sekerka, Stability of planar interface during solidification of a dilute binary alloy, *J. Appl. Phys.* **35**, 444–451 (1964).
20. L. A. Tarshis, S. O'Hara and R. Viskanta, Heat transfer by simultaneous conduction and radiation for two absorbing media in intimate contact, *Int. J. Heat Mass Transfer* **12**, 333–347 (1969).
21. M. N. Ozisik, *Radiative Transfer and Interactions with Conduction and Convection*, p. 416. Wiley, New York (1973).

EFFETS DU TRANFERT RADIATIF INTERNE SUR LA CONVECTION NATURELLE ET LE TRANSFERT THERMIQUE DANS LA CONFIGURATION DE CROISSANCE VERTICALE D'UN CRISTAL

Résumé—On examine l'effet du rayonnement interne sur le processus de croissance d'un cristal unique. Un modèle bidimensionnel de croissance verticale est utilisé pour simuler la méthode verticale de Bridgman. L'approximation différentielle est utilisée pour modéliser le transfert radiatif sur une base spectrale et prendre en compte les interactions entre le cristal et le bain. Des conditions aux limites pour les cristaux semi-transparents sont développées pour couvrir le domaine entre opaque et transparent. Les équations sont résolues numériquement par une méthode aux différences finies. Les solutions montrent une réduction notable de la différence de température près de l'interface cristal-bain et de l'intensité de la convection naturelle dans le bain, avec la décroissance de l'opacité du cristal. Les calculs montrent qu'il y a une petite différence relative entre les prédictions de bande spectrale et celles du modèle gris basé sur un coefficient d'absorption moyen géométrique. Les résultats obtenus indiquent la nécessité de considérer le rayonnement thermique pour améliorer la précision des modèles qui simulent la croissance d'un cristal.

EINFLUSS DER INNEREN STRAHLUNGSWÄRMEÜBERTRAGUNG AUF DIE NATÜRLICHE KONVEKTION UND DEN WÄRMEÜBERGANG IN EINER SENKRECHTEN ANORDNUNG FÜR DAS KRISTALLWACHSTUM

Zusammenfassung—In dieser Arbeit wird der Einfluß einer inneren Strahlungswärmeübertragung auf den Vorgang des Wachstums eines Einkristalls untersucht. Ein zweidimensionales Modell der senkrechten Anordnung für das Kristallwachstum wird verwendet, um das senkrechte Bridgman-Verfahren zu simulieren. Die Strahlungswärmeübertragung wird mit Hilfe der differentiellen Approximation auf spektraler Grundlage modelliert, dabei werden Wechselwirkungen innerhalb des Kristalls und der Schmelze berücksichtigt. Es werden Randbedingungen für halbtransparente Kristalle entwickelt, welche den Bereich vom völlig Undurchsichtigen bis zum Transparenten abdecken. Die Grundgleichungen werden numerisch mit Hilfe eines Finite-Differenzen-Verfahrens gelöst. Die Lösungen zeigen eine merkliche Verringerung der Temperaturdifferenz nahe der Grenzfläche zwischen Kristall und Schmelze und ebenso eine Verringerung der Intensität der natürlichen Konvektion in der Schmelze, wenn von einem völlig undurchsichtigen Kristall abgewichen wird. Es zeigt sich, daß die Strahlung von der Seitenwand die Struktur der natürlichen Konvektion in der Schmelze beeinflußt. Die Berechnungen ergeben einen verhältnismäßig kleinen Unterschied zwischen Berechnungen mit Berücksichtigung unterschiedlicher Spektralbereiche einerseits und Berechnungen grauer Körper aufgrund geometrisch gemittelter Absorptionskoeffizienten andererseits. Als Ergebnis kann festgehalten werden, daß interne Strahlungswärmeübertragung berücksichtigt werden muß, wenn man zu einer Verbesserung der Genauigkeit von Modellrechnungen für das Wachstum von Einkristallen kommen möchte.

ВЛИЯНИЕ ВНУТРЕННЕГО РАДИАЦИОННОГО ПЕРЕНОСА НА ЕСТЕСТВЕННУЮ КОНВЕКЦИЮ И ТЕПЛООБМЕН В ПРОЦЕССЕ РОСТА КРИСТАЛЛА ВЕРТИКАЛЬНОЙ КОНФИГУРАЦИИ

Аннотация—Исследуется влияние внутреннего излучения на процесс роста кристалла. Используется двумерная модель роста кристалла для вертикального метода Бриджмэна. С целью моделирования радиационного теплопереноса и его взаимодействия с кристаллом и расплавом применяется дифференциальное приближение, а также учитывается спектральный состав излучения. Установлены граничные условия для полупрозрачных кристаллов в диапазоне от непрозрачных до прозрачных. Определяющие модельные уравнения численно решаются методом конечных разностей. Решения показывают, что разность температур вблизи границы раздела кристалла и расплава, а также интенсивность естественной конвекции в расплаве заметно убывают при уменьшении непрозрачности кристалла. Найдено, что излучение от обковой стенки является фактором, влияющим на структуру течения при естественной конвекции в расплаве. Расчеты обнаружили относительно небольшую разницу между данными, полученными методом спектральных полос, и результатами расчета на основе серой модели с использованием геометрического среднего коэффициента поглощения. Полученные результаты указывают на необходимость исследования внутреннего радиационного теплопереноса для повышения точности моделей роста кристалла.